

Inverse Mapping of Pulsar Magnetospheres: Optical Emission Comes From 300 km Above the Surface

Diarmaid de Búrca, Pádraig O'Connor, John McDonald
and Andy Shearer

Centre for Astronomy, National University of Ireland, Galway
email: diarmaiddeburca@gmail.com

Abstract. In order to determine the emission height of the optical photons from pulsars we present an inverse mapping approach, which is directly constrained by empirical data. The model discussed is for the case of the Crab pulsar. Our method, which uses the optical Stokes parameters, determines the most likely geometry for emission including the magnetic-field inclination angle (α), the observer's line-of-sight angle (χ) and emission height. We discuss the computational implementation of the approach, and the physical assumptions made. We find that the most likely emission altitude is at 20% of the light-cylinder radius above the stellar surface in the open field region.

Keywords. pulsars: general, polarisation

1. Introduction

Even after more than 40 years of observation and theory about pulsar emission, there is still no consensus as to how and where it occurs. There is a general agreement that the energy comes from the slowing down of the pulsar caused by some kind of dipole braking, but there is no accord as to where in the magnetosphere the emission occurs. While recent gamma-ray observations of radio-quiet pulsars have effectively ruled out a polar-cap model (Abdo *et al.* 2009), there are still the outer gap, the slot-gap and the 2-pole caustic models to be considered.

One of the main problems with modelling pulsars is that the emission is heavily dependent on the geometry, and that geometry is usually unknown. In this work we consider the geometry of the pulsar as an additional parameter to be fitted. Light curves are plotted for a range of different viewing angles and inclination angles and are then compared to observation. Once a best fit to observation has been obtained, an inverse mapping approach is used to locate the emission sites.

2. Assumptions

In order to build our model, some simple assumptions were made:

- The optical emission is a synchrotron process
- The magnetic field is in the form of a retarded dipole (Michel & Li 1999)
- The open field region is fully populated with radiating electrons

Starting from those assumptions, we calculated the light curves emitted on the basis of a number of parameters—the orientation of the magnetic-field axis, the electron pitch angle distribution and cut-off, and the observer's viewing angle.

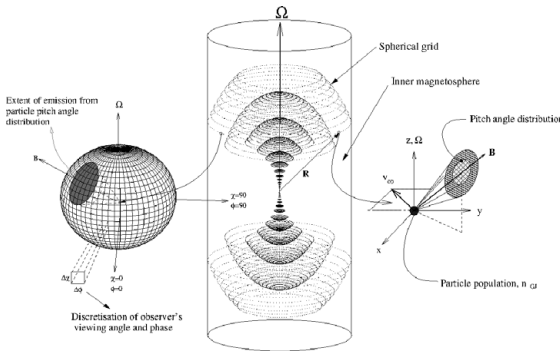


Figure 1. Centre: The concentric spherical Cartesian grid imposed on the pulsar magnetosphere, showing only points in the open magnetosphere. Right: At each individual location (\mathbf{R}) we calculate the radiation emitted from the local particle distribution, taking the local physical conditions into account (e.g., \mathbf{B} , v_{co} , the power law distribution, etc). Left: Representation of how emission from a particle pitch-angle distribution (PAD) extends over a range of viewing angles χ and phase Φ . Emission is recorded computationally in discrete bins of length $\Delta\chi$ and $\Delta\Phi$.

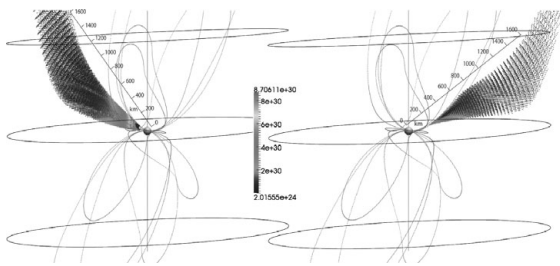


Figure 2. 3-D representation of the regions contributing to the emission in the main peak (left) and to the secondary peak (right), for a model (Crab) pulsar with parameters $(\alpha, \chi, PAD, PAD_{co}) = (80, 25, \text{isotropic}, 20)$. The intensity scale shows the emission contributions in the regions mapped. The circles define the light cylinder boundary and the lines are the open volume/closed volume boundary. The emission is seen to be concentrated in the lower magnetosphere from a single pole.

A full description of the model we used can be found in McDonald *et al.* (2011). We constrain our model by comparing the output with observation (all Stokes parameters).

3. Results

Currently we compute all Stokes parameters and compare them against the observations. To date there have been no observations of circular polarisation from the Crab pulsar, so our constraints are limited to intensity and linear polarisation. Inverse mapping results are given for a selected (α, χ) combination, which compared most favourably with the double-peaked structure of the Crab light curve. Values of $(\alpha, \chi) = (70^\circ, 45^\circ)$ with a $(PAD, PAD_{co}) = (\text{isotropic}, 45^\circ)$ were chosen. Our preferred values of α and χ were broadly consistent with Ng & Romani (2000), who provided a robust estimate of the Crab inclination angle.

The inverse mapping approach enables us to decompose light curves, with the option of selecting different phase-resolved regions which can then be traced back into the magnetosphere, thereby isolating the emission locations of individual photons. That then localises the magnetospheric emission sites which contribute to the emission at a particular phase. We attempt here to present the results of that inverse mapping in 3 dimensions, though it is not an easy task. In Fig. 3 we present an intensity map of the emission locations. On the left are emission sites for the main pulse while on the right are the emission sites from the secondary pulse. One thing of immediate note is that the emission appears to be coming from one pole (pole one) for the peak, but from the opposite pole for the inter-pulse.

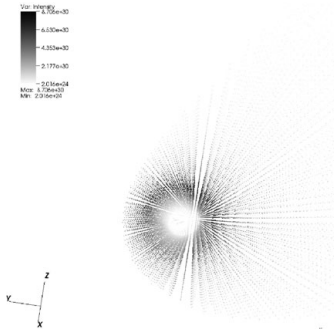


Figure 3. 3-D representation of emission sites from the Crab pulsar for the main peak, at viewing angle of 52° and inclination angle of 70° . As can be seen, there is a ring of high-energy emission. This ring appears to be following the last open field lines, in concordance with the slot-gap model.

4. Conclusions

Optical polarisation studies can be used to determine the local geometry of the emission region. In particular, from this work we see that a simple synchrotron model gives good agreement with observation. The linear polarisation peaks on the rising edge of the main pulse, in agreement with Smith *et al.* (1988) and Słowikowska *et al.* 2009. We find that, for the most part, the radiation is circularly polarised, with an interplay between circular and linear polarisation occurring on the rising edge of the main peak. On that basis, observations of the circularly polarised optical emission from pulsars should provide significant geometrical constraints to the pulsar parameters, though we accept that more detailed work is required in order to define more realistic emission locations.

Our model predicts that the pulsar emission is low in the magnetosphere (roughly 300 km from the star). That is some distance from the regions predicted by most models, with the slot-gap model being the nearest. Our model also predicts a ring of high-energy emission from the region around the last open field lines, again supporting the slot-gap model, as seen in Fig. 3.

Our future work will entail restricting the emission to locations around the last open field lines, thereby removing the inherent symmetry of the model. In that way we hope to make firmer predictions about the optical emission specifically, and to comment more generally on the correlations between optical and radio emission (Słowikowska *et al.* 2009). Furthermore, we will tune our inverse mapping constraints to intensity alone, e.g., for comparison with gamma-ray light curves.

As well as giving the emission location and pulsar orientation, our model can also constrain the PAD and the PAD_{co} . We intend to make a more detailed comparison between our model and circularly-polarised emission. To date there have not been any measurements of optical circular polarisation from any pulsar. A new instrument, the Galway Astronomical Stokes Polarimeter, has that capability, and observations of the Crab pulsar are planned for late 2011.

References

- Abdo, A. A., *et al.* 2009, *Sci*, 325, 848
 McDonald, J. O'Connor, P., de Búrca, D., Golden, A., & Shearer, A., 2011, *MNRAS*, 417, 730
 Michel, F. C. & Li, H. 1999, *Phys. Reports*, 318, 227
 Smith, F. G., Jones, D. H. P., Dick, J. S. B. & Pike, C. D. 1988 *MNRAS*, 233, 305
 Słowikowska, A., Kanbach, G., Kramer, M., & Stefanescu, A. 2009 *MNRAS*, 397, 103
 Ng, C.-T., Romani, R. 2000 *ApJ*, 601, 479